Contextual LCIA Without the Overhead: An Exchange-based Framework for Flexible Impact Assessment

Romain Sacchi[1,2*], Alvaro Hahn Menacho[1,2], Georg Seitfudem[3], Maxime Agez[3], Joanna Schlesinger[4], Anish Koyamparambath[5], Jair Santillan Saldivar[6], Philippe Loubet[5], Christian Bauer[1]

[1] PSI Centers for Nuclear Engineering and Sciences and for Energy and Environmental Sciences, Paul Scherrer Institute, Villigen, Switzerland
[2] Chair of Energy Systems Analysis, Institute of Energy and Process Engineering, ETH Zürich, Zürich, Switzerland
[3] CIRAIG – Department of Chemical Engineering, Polytechnique Montréal, Montréal, Canada
[4] Centre Observation, Impacts, Energie, Mines Paris – PSL, Sophia Antipolis, France
[5] Université de Bordeaux, CNRS, Bordeaux INP, ISM, UMR 5255, F-33400, Talence, France
6 BRGM, BP 36009 45060 Orléans Cedex 2, France
* Corresponding author : romain.sacchi@psi.ch

Abstract

Purpose: Life Cycle Impact Assessment (LCIA) has traditionally applied characterization factors (CFs) to elementary flows (nodes) in isolation, treating impacts as fixed properties of substances, regardless of where and how they occur within the life cycle network. While recent advances have introduced regionalized LCIA methods and GIS-based spatial modeling frameworks, these remain difficult to operationalize in routine assessments and are often limited to node-level differentiation. This paper presents a methodological advancement in LCIA: the application of CFs at the level of edges—the resolved biosphere and technosphere flows between processes.

Methods: Shifting the CF unit from nodes to edges enables CFs to reflect the full context of each exchange, including the geographic origin and destination, the identity of the supplier and consumer, and prospective, scenario-dependent parameters. The method offers a flexible, intermediate solution between

traditional node-based LCIA and full spatially explicit models, supporting national and subnational regionalization without requiring high-resolution GIS integration.

Results: The approach is implemented in the open-source Python library *edges*, which extends the *Brightway* LCA framework to support context-sensitive and symbolic CFs. We illustrate its capabilities through four applications: 1) Regionalized LCIA, using the AWARE water scarcity method with dynamic handling of region aggregation and disaggregation; 2) Technosphere-based LCIA, via a new implementation of the GeoPolRisk indicator, which assigns CFs based on country-to-country commodity trade relationships; and scenario-sensitive prospective LCIAs, enabling alignment with climate scenarios, where CFs are defined by symbolic expressions that depend on scenario-specific variables, with application 3) focusing on global warming potential based on atmospheric gas concentration, and application 4) addressing fossil resource scarcity through dynamic fossil fuels extraction rates.

Conclusions: Together, these examples demonstrate how exchange-resolved LCIA expands the methodological space of impact modeling, offering a scalable, context-aware framework for regional, relational, and future-oriented life cycle assessments.

1 Introduction

Life Cycle Impact Assessment (LCIA) translates emissions and resource use into environmental impacts by applying characterization factors (CFs). Traditionally, CFs are applied to elementary flows at the node level—that is, to substances such as "carbon dioxide, fossil" or "water, from well"—regardless of the flow's context within the life cycle network. This conventional approach treats impacts as inherent properties of elementary flows, detached from the relationships that cause them.

Over the past two decades, efforts to improve the spatial representativeness of LCIA have led to the development of regionalized methods, such as EDIP2003 (Hauschild and Potting 2005), Accumulated Exceedance (Seppälä et al. 2006), AWARE (Boulay et al. 2018), ImpactWorld+ (Bulle et al. 2019), and LC-IMPACT (Francesca Verones et al. 2020). These approaches assign CFs to specific regions (e.g., countries, grid cells, or even watersheds), allowing LCIA to account for spatial variability in fate, exposure, or vulnerability. However, integrating such methods into full life cycle studies has remained a challenge, as CFs are still typically applied to aggregated biosphere flows, after the resolution of the inventory has discarded crucial contextual information.

A common workaround LCA software (e.g., Simapro, OpenLCA) adopted has been introducing region-specific elementary flows—such as creating separate flows like "Water, DE" or "Water, FR" to represent country-specific water withdrawals. This approach allows geographically differentiated CFs to be applied within node-based frameworks. However, it is inherently inefficient and unscalable. Representing global spatial variability would require duplicating elementary flows relevant to the impact assessment method for potentially hundreds of regions, leading to a proliferation of flows, increased database complexity, and a higher risk of manual and systemic modeling errors. Moreover, this strategy treats geographic information as part of the flow (node) identity rather than as a separate, context-dependent exchange (edge) attribute.

A key step toward addressing these limitations was proposed by Mutel & Hellweg (2009), introducing a computational framework for applying region-specific CFs across extensive inventories by matching the geographic metadata of emitting processes before inventory aggregation. This advance made it possible to conduct regionalized LCIA using only the location data already embedded in life cycle databases. Mutel et al. (2012) further extended this

framework by introducing geographic information system (GIS)-based tools to bridge mismatched spatial units between inventories and CFs, proposing spatial mapping matrices and methods for assessing uncertainty and spatial resolution. Together, these studies established the feasibility of integrating geographic structure into LCA workflows in a systematic way.

Yang & Heijungs (2017) generalized this approach further by proposing a multi-regional algebraic formulation of LCA, where both the technosphere and biosphere matrices are indexed by region. Their model captured where emissions occur and how materials and impacts are transferred across space, highlighting the need to account for relational structure (i.e., trade) in regionalized assessments.

More recently, Li et al. (2021) proposed a universal GIS-LCA framework based on an extensive literature review, emphasizing consistent spatial referencing and a harmonized geospatial layer across all phases of LCA. Their vision supports full spatial traceability—potentially down to high-resolution grids—but assumes access to GIS data, spatial overlays, and detailed geographic inventories.

While these contributions have significantly advanced the field, they illustrate a methodological spectrum—from fully generic, location-neutral LCIA to spatially explicit, GIS-integrated models. However, fully generic approaches—where CFs are applied to elementary flows without spatial or contextual differentiation—can obscure significant regional or sectoral variations. Conversely, highly detailed GIS-based models, although scientifically robust, often require data and computational resources that limit their practical adoption, as evidenced by their limited uptake in current LCA practice. Our work offers a pragmatic intermediate solution along this spectrum. We propose a generalization of LCIA that shifts the focus from so-called "elementary flows" (e.g., "Water, from lake") to consider instead exchanges (e.g., "Water, from lake → maize grain production {US}"), treating the edge between the supplying and consuming node as the unit of impact characterization. In this exchange-based approach, CFs can be defined not only by the flow's substance and quantity, but also by: 1) the location of both supplying and consuming nodes (supporting national and subnational regionalization); 2) the identity or type of actors involved (e.g., industrial classification, activity type); and 3) external parameters or scenarios, such as climate policy targets or atmospheric composition. Practical examples of such a framework include differentiating impacts from water use for agricultural and industrial purposes, and further refining the CF selection based on the consuming process's location. Another example is to link an exchange to a parameterized CF, such as the global warming impact of methane as a function

of its atmospheric concentration, which is defined by a scenario. These examples, and others, are further detailed throughout this work.

This method captures more context than node-based models while avoiding the complexity and data intensity of GIS-based LCIA. It supports regionalized LCIA with national and subnational resolution. Still, it does not depend on fine-grained spatial data or GIS layers as input, making it more accessible and scalable for routine assessments.

Moreover, exchange-based LCIA transcends geographic differentiation. It allows CFs to rely on technosphere structure (e.g., supply chains, country-to-country flows) and be represented as symbolic functions of external parameters, facilitating scenario- and policy-sensitive assessments.

These capabilities are implemented in the open-source Python library *edges*, which integrates with the *Brightway* framework (Mutel 2017). While tools like *brightway2-regional* focus on region-matching for biosphere flows using GIS, *edges* enables exchange-specific CFs across both the biosphere and technosphere, parameterized or symbolic CFs, and a modular mapping system for handling aggregated (e.g., "RER") or dynamic regions such as "RoW" (Rest of the World) and "RoE" (Rest of Europe).

We demonstrate the methodological potential of this approach through four illustrative applications: 1) Regionalized LCIA, using the AWARE method for water scarcity impact assessment, with logic for disaggregating and aggregating exchanges by region. 2) Technosphere-aware LCIA, via a new implementation of the GeoPolRisk indicator (Koyamparambath et al. 2024), where impacts depend on the origin-destination pair in resource supply chains. Finally, two scenario-based prospective LCIA applications: 3) the use of symbolic characterization factors for CH_4 and N_2O that dynamically respond to scenario-specific atmospheric concentrations and time horizon parameters, and 4) the recalculation of surplus fossil fuel production costs based on projected extraction volumes and marginal costs.

Although the approach primarily draws on foundational insights from Mutel & Hellweg (2009) and, to some extent, those of Mutel et al. (2012) and Yang & Heijungs (2017), it introduces a novel modeling layer that enables context-aware, exchange-level impact assessment—without the overhead of full GIS in-tegration. In doing so, it helps bridge the gap between theoretical advances in spatial modeling and practical applications in prospective and regionalized LCA.

In the following sections, we present the technical foundations of exchange-resolved LCIA, describe the *edges* implementation, and illustrate its application in the four domains mentioned above.

2 Method

Traditional LCIA applies CFs to elementary flows using either a vector or a diagonal matrix, where each flow (e.g., "Water, from lake") is assigned a single CF that remains invariant to context. Consequently, this structure cannot differentiate between the same substance emitted in different regions or flows arising from various supply chain relationships.

We propose an approach in which CFs are assigned at the level of exchanges—the directed links between supplying and consuming nodes in the LCI graph. Each exchange includes information such as flow quantity, information about the supplying and consuming nodes, such as the matrix they belong to (biosphere or technosphere), and their respective location, if relevant. Together with other optional scenario parameters (e.g., CO_2 concentration, time horizon), this information can be used to apply CFs that better fit the context of the exchange.

2.1 Node vs. Edge-based LCIA

In conventional LCIA, the impact vector h for a given functional unit is computed using the standard matrix formulation (Heijungs and Suh 2002):

$$h = Q \cdot B \cdot A^{-1} \cdot f$$

where:

- f $(p \times 1)$ is the functional unit vector, or demand vector;
- A $(p \times p)$ is the technosphere matrix;
- B $(q \times p)$ is the biosphere matrix;
- Q $(q \times 1)$ is a vector of CFs, one per elementary flow;
- And h is the impact vector.

This formulation is equivalent to the matrix product:

$$h = 1^T \cdot Q \cdot X \cdot f$$

where:

- $X\ (q \times p) = B \cdot A^{-1}$ is the inventory matrix, where each column corresponds to a process and each row to an elementary flow
- $Q = diag(c)$, a diagonal matrix of CFs

In our exchange-resolved LCIA approach, we instead apply a non-diagonal, rectangular CF matrix, referred to as $E(q \times p)$, to the full inventory matrix $X\ (q \times p)$, characterizing each flow per activity, to obtain the impact matrix H:

$$H = \sum_{i=1}^{q} \sum_{j=1}^{p} E_{ij} \cdot X_{ij} = \sum (E \circ X)$$

This formulation enables the same elementary flow to receive different CFs depending on:

- The supplying node attributes (e.g., its location, activity classification code, unit, associated matrix type);
- The consumer node attributes (same as above);
- Any external parameters included in CF definitions (e.g., concentration, time horizon, amount emitted).

It generalizes the conventional LCIA formulation by allowing each exchange to be characterized uniquely, and serves as a foundation for flexible impact modeling.

The exchange-resolved method also enables the characterization of technosphere exchanges—i.e., intermediate flows between activities. This is particularly relevant for indicators relating to supply risks (e.g., GeoPolRisk), where impacts depend on the supply chain relationships between countries or sectors. To support this, we construct a technosphere exchange matrix, T (p x p), that represents the quantity of each intermediate product exchanged between activities. This matrix is derived from the technosphere matrix A and the supply array s. The latter represents the scaling of each activity required to meet the functional unit:

$$T = (-A \circ M) \cdot diag(s)$$

where:

- $M \in \{0, 1\}^{p \times p}$ is a binary mask matrix where $M_{ij} = 1$ if $A_{ij} < 0$, and 0 otherwise,
- $diag(s)$ is a diagonal matrix of the supply array s, defined as $s = A^{-1} \cdot f$.

The characterization step is similar to that of characterizing biosphere exchanges:

$$H = \sum_{i=1}^{q} \sum_{j=1}^{p} E_{ij} \cdot T_{ij} = \sum (E \circ T)$$

Hence, compared to traditional LCA terminology, this framework expands the meaning of "characterization factor" to allow for the characterization of technosphere flows.

2.2 Exchange matching

Definitions of CFs are matched to exchanges using criteria that enable the identification of specific supplying-consuming node pairs, such as:

- Node name or substring (e.g., "Water")
- Node matrix (biosphere or technosphere)
- Node metadata (e.g., location, classification)

This logic applies to supplying and consuming nodes, allowing directional differentiation (e.g., CFs specific to Swiss exports to Germany).

To support regionalized LCIA, exchanges are mapped to CF regions through:

- Direct matching (this includes matching to aggregated regions such as "Asia" or "RER");
- Association: the CF of a region, if missing, is defined as the CF of the closest matching region (i.e., usually a region that contains it, e.g., “Canada” for “Québec”);
- Dynamic resolution: the CF for relative regions (e.g., RoW) is computed based on uncovered areas. A weighted average CF is calculated from the CF of all non-overlapping regions, excluding those for which region-specific inventories exist;
- Fallbacks: if no regional match is found, unmatched exchanges receive a global average CF.

For composite regions, CFs can be calculated on-the-fly and with dynamic extent: CFs for composite inventory regions (e.g., "RER") are calculated as the weighted average of the CFs of the areas they comprise, using weighting keys such as resource consumption, population, or GDP, or any other weighting key provided by the LCIA method.

The weighting key can vary in cases of association, aggregation, and dynamic resolution, depending on the population, country-level emissions, resource consumption, or GDP. For example, in the case of AWARE 2.0, the national water demand in 2019 is used.

2.3 Characterization factors evaluation

Characterization factors are evaluated dynamically and inserted into the characterization matrix E before obtaining the characterized inventory matrix H. The value of the CF can be:

- Numeric (e.g., 28)
- Symbolic (e.g., "28 * (1 + 0.001 * (co2ppm - 410))"), with *co2ppm* being a parameter with its value changing across scenarios
- Supplied externally via a function call

2.4 Software Implementation: The edges Python Library

The method presented in this paper is implemented in the open-source Python library *edges*. Built on the Brightway framework, *edges* enables exchange-resolved LCIA by applying CFs directly to inventory exchanges using flexible matching rules, as described above.

Characterization factors can be defined in JSON or programmatically, and worked examples are available in the online repository. *Edges* is released under the MIT license and is actively maintained by PSI. At the time of writing, *edges* implements regionalized factors for AWARE 2.0, IMPACT World+ 2.1, and GeolPolRisk 1.0.

2.5 Examples

The Results section presents four use cases to illustrate the exchange-resolved characterization approach. They highlight different capabilities of the method: regionalization, technosphere-based modeling, and scenario-based prospective assessment. The first two use cases have a current reference year (2025), while the two last use cases are evaluated from 2020 to 2100. For each of the four cases, hydrogen production is modeled using Proton Exchange Membrane (PEM) water electrolysis. Inventories are based on Gerloff (2021), adapted to a French context and receive an input of offshore wind power from the ecoinvent 3.10.1 cut-off database (Wernet et al. 2016) – see Table 1. The resulting environmental burdens are entirely allocated to the produced hydrogen; oxygen, the other output of the water electrolysis process, is assumed to be released to the atmosphere and thus considered a by-product with an economic value of zero. Inventories are available as part of the electronic SI material. While energy storage would ideally be included to account for the intermittency of the offshore wind supply, it is omitted here for simplicity. This omission does not affect the validity of the findings illustrated in the use cases.

Table 1: Inventories for producing one kilogram of hydrogen with water electrolysis using a PEM electrolyzer. Original source: 1 MW PEM electrolyzer by Gerloff (2021). Lifetime and efficiency are further refined with data from the manufacturer's specifications and the InDWEDe project report (Smolinka et al. 2018). A water consumption of 14 liters per kg of hydrogen is assumed (Simoes et al. 2021), which accounts for losses due to evaporation and cleaning. Ultrapure water treated by a single pass reverse osmosis was modelled using inventories from (Gonzales-Calienes et al. 2022).

Process	Hydrogen production, gaseous, 30 bar, from PEM electrolysis, using offshore wind power			
Reference product	Hydrogen, gaseous, 30 bar			
Location	FR			
Unit	Kilogram			
Exchanges				
Name	Quantity	Location	Unit	Reference product
	Output			
hydrogen production, gaseous, 30 bar, from PEM electrolysis, from grid electricity	1.00E+00	FR	Kilogram	hydrogen, gaseous, 30 bar
Oxygen	8.00E+00		Kilogram	
	Inputs			

electrolyzer production, 1MWe, PEM, Stack	1.35E-06	RER	Unit	electrolyzer, 1MWe, PEM, Stack
electrolyzer production, 1MWe, PEM, Balance of Plant	3.37E-07	RER	Unit	electrolyzer, 1MWe, PEM, Balance of Plant
treatment of electrolyzer stack, 1MWe, PEM	-1.35E-06	RER	Unit	used fuel cell stack, 1MWe, PEM
treatment of electrolyzer balance of plant, 1MWe, PEM	-3.37E-07	RER	Unit	used fuel cell balance of plant, 1MWe, PEM
electricity production, wind, 1-3MW turbine, offshore	5.40E+01	FR	Kilowatt-hour	electricity, high voltage
deionized water production, via reverse osmosis, from river	1.40E+01	FR	Kilogram	water, deionized
Occupation, industrial area	6.07E-04		Square meter·year	
Transformation, from industrial area	3.04E-05		Square meter	
Transformation, to industrial area	3.04E-05		Square meter	

2.5.1 Use Case 1: Regionalized LCIA with AWARE

The first example focuses on regionalized LCIA using the AWARE 2.0 water scarcity LCIA method (Boulay et al. 2018; Seitfudem et al. 2025). The indicator assesses the potential impacts of water consumption on other water users. Its core variable estimates the relative amount of water remaining in a watershed after human and ecosystem demands are met, expressing results as a scarcity-weighted water consumption factor. AWARE CFs at the watershed level with a monthly resolution are a generic indicator of the potential to deprive other water users of water. AWARE's applicability is enhanced by spatially aggregated annual factors, such as for entire countries. The current implementation of AWARE 2.0 in *edges* includes 512 unique CFs. Since they are spatiotemporal aggregations, they reflect the geographic context of freshwater consumption and the consumption pattern, both spatially and temporally. The following example specifies the CF for freshwater uptake in Armenia (ISO country code: "AM"):

```
{
    "supplier": {
       "name": "Water, lake",
       "categories": [
```

```
            "natural resource",
            "in water"
         ],
         "matrix": "biosphere"
      },
      "consumer": {
         "location": "AM",
         "matrix": "technosphere",
         "classifications": {
            "CPC": [
               "01"
            ]
        }
      },
      "value": 88.6,
      "weight": 799882000,
      "uncertainty": {
         "distribution": "discrete_empirical",
         "parameters": {
            "values": [
               84.5,
               87.9
            ],
            "weights": [
               0.031,
               0.969
            ]
        },
        "negative": 0
    }
}
```


This definition assigns a CF of 88.6 m^3 world-eq./m^3 freshwater to any exchange where the supplying node belongs to the biosphere matrix and is labeled "Water, lake" (in the "natural resource" compartment), and the consuming node is a technosphere process situated in Armenia.The Central Product Classification (CPC) field value “CPC: 01” indicates that this CF only applies to consumers with the corresponding CPC category (i.e., “01” relates to agricultural activities). Aiming for closer representing the spatiotemporal distribution of water consumption in CF aggregations, AWARE provides different aggregated factors for agricultural and non-agricultural activities. High spatiotemporal heterogeneity is typical for the water consumption of agricultural activities, with irrigation often being limited to a few months. For the annual averages presented in Armenia’s example above, watersheds and months are consequentially weighted by irrigation water consumption. In the same fashion, *edges* provides AWARE CFs for non-agricultural activities and activities for which the type cannot be determined. Hence, exchanges are not only discriminated against based on the consumer's location but also the consumer's type (i.e., seasonality and spatial pattern of water consumption in this case).
The weight field provides a reference freshwater consumption volume for the area (annual, in m^3/year), used when aggregating or disaggregating regional

CFs—e.g., to compute weighted averages for larger or composite regions (e.g., RER, RoW).

In addition to the spatial and sectoral resolution of the CFs, the method supports the representation of uncertainty or variability ***via*** probability distributions. Each CF can be supplemented with an uncertainty field, which describes the statistical distribution of potential CF values rather than relying on a single deterministic point estimate. Several types of distributions are supported, including normal, lognormal, gamma, beta, triangular, uniform, and discrete empirical. These distributions are defined by standard parameters (e.g., mean, scale, shape, minimum, maximum) and are used for Monte Carlo sampling to generate pseudo-random values for error propagation. In the example above, the spatial variability of watersheds within a country is represented using the "discrete_empirical" distribution. This approach is particularly well-suited for watershed-specific CFs derived from multiple data sources or seasonal profiles. Rather than assuming a continuous parametric distribution, the discrete empirical type defines a set of possible CF values (corresponding to the individual watersheds of the region) and their associated weighted probabilities of providing water. In this case, the two watersheds of Armenia are associated with two CF values—84.5 and 87.9—each given a respective weight of 3.1% and 96.9%, based on the respective watersheds' annual irrigation water consumption. When sampling during LCIA, one of these values is drawn according to its likelihood, allowing for the capture of spatial and seasonal variability or model uncertainty (when available) without imposing an arbitrary statistical shape. In this case, the risk would be, in regions with a limited number of watersheds, to draw CF values for watersheds that do not exist. However, note that this example does not account for the inherent uncertainty of the CF value for a specific watershed, as AWARE 2.0 does not yet carry uncertainty data. Rather, it considers the uncertainty as to which watershed will provide freshwater to the consuming process within a country. For other regions that comprise numerous watersheds (i.e., n>10), parametric distributions have been fitted, such as the case of California (see Fig. 1). When aggregated to form regional or global indicators, these probability distributions contribute to a more robust and transparent impact assessment. However, two main limitations of this approach are worth discussing: 1) It is currently unable to calculate probability distributions for composite regions (e.g., RoW). 2) To capture spatial variability in watershed-level CFs while maintaining LCA robustness (Mutel et al. 2019), we aggregate CFs from watersheds to regions in *edges*. However, this can reduce precision for smaller regions—e.g., certain

Indian and U.S. states—where seasonal water use patterns in the region-specific portion of a watershed differ from the watershed as a whole. In 59 regions, over half of water consumption showed >10% discrepancy between the annual watershed CF and the (unpublished) annual CF of the watershed's region-specific portion. In such cases, we opted for deterministic AWARE values instead of Monte Carlo sampling. This issue stems from using annual rather than monthly CFs, reflecting a modeling constraint rather than a limitation of the AWARE method.

Furthermore, although not used here, *edges* also supports *nested* distributions: for example, had uncertainty data at the watershed level been available, it could have been combined with a discrete distribution. Hence, at the country level, a watershed would be picked according to consumption-weighted probabilities, and after that, pseudo-random values would be drawn from the watershed-specific distribution.

Finally, to ensure consistent uncertainty treatment for correlated flows (such as water uptake and release in the same location), *edges* generates shared sampled vectors for each unique CF distribution. This preserves correlation between exchanges, such as when a water flow appears as both an input and output (e.g., in water use modeling). For instance, in the hydrogen system, two exchanges—"Water, surface water" (i.e., release) and "Water, natural resource in water" (i.e., uptake) point to a consuming node located in the United Arab Emirates. They share the same discrete empirical distribution (since the water is withdrawn and released in the same region), with possible watershed-specific values like 7.56, 13.4, 33.7, etc. By caching a single sample vector (e.g., [27.6, 7.56, 33.7, ...]) and applying signs only after sampling, we ensure they receive the same values in the same order, respecting their contextual direction (i.e., consumption or release), before being multiplied by the exchange amount. This avoids decorrelation artifacts in Monte Carlo analyses and enables reliable uncertainty propagation across symmetrical exchanges.

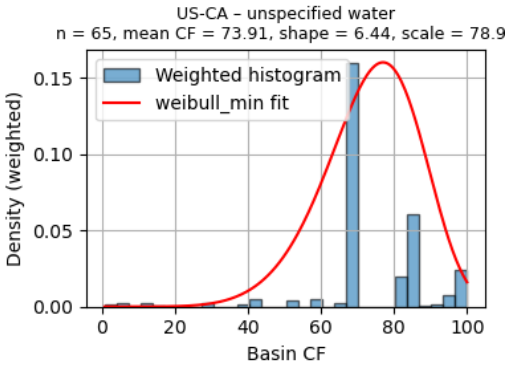

Fig. 1 – Fitted parametric distribution over the watershed-specific CF values for California, USA, for unspecified water consumption type. It is a Weibull distribution of mean 73.9 fitted over the CFs of 65 watersheds.

2.5.2 Use Case 2: Technosphere-based LCIA with GeoPolRisk

The second use case demonstrates how exchange-resolved LCIA can be extended beyond biosphere flows to characterize technosphere exchanges—i.e., intermediate product flows between activities. We illustrate this using the GeoPolRisk indicator (Gemechu et al. 2016; Koyamparambath et al. 2024). The indicator quantifies the geopolitical risks associated with the extraction of mineral resources. It assigns characterization factors based on the likelihood and severity of supply disruptions in producing countries due to political instability, conflict, or governance issues.

Initially, GeoPolRisk CFs were applied to raw material elementary flows (Koyamparambath et al., 2024), limiting the ability to account for the geographic locations of resource suppliers and consumers. Moreover, elementary flows do not necessarily represent the marketable materials at risk. This stems from (i) the pre-allocation of multi-output mining processes in databases such as ecoinvent, which can create imbalances between elementary and intermediate product flows for a given material, as well as (ii) losses during processing stages. The *edges* method addresses both limitations by applying location-specific CFs directly to technosphere exchanges. GeoPolRisk CFs were extended to the intermediate product level using the *geopolrisk-py* library (Koyamparambath et al., 2024), which enables the generation of country-to-country CFs. Those were then mapped to ecoinvent's nomenclature. Hence, the method offers CFs based on country-to-country trade relationships of abiotic resources in its detailed form.

An example CF definition is shown below:

```
{
  "supplier": {
    "name": "aluminium production",
    "reference product": "aluminium",
      "location": "AU",
      "operator": "startswith",
      "matrix": "technosphere",
      "excludes":[
        "alloy",
        "liquid",
        "market"
        ]
  },
  "consumer": {
      "location": "CA",
      "matrix": "technosphere"
  },
  "value": 2.420e-4
}
```

This CF definition assigns a supply risk value, expressed in kg copper-eq./kg, to exchanges where primary aluminium is supplied by Australia ("AU") and consumed in Canada ("CA"). The CF reflects the geopolitical risk associated with this specific supply route for this metal. The same metal, consumed by Canada but supplied instead by the United States (“US”), is given a CF value 10 times higher. This indicates that a disruption in the “US” supply would have more severe consequences for Canada, given its greater dependence on aluminium imports from the United States.
Here, the operator "startswith" and the “excludes” list allow for pattern-based matching of activity names, offering flexibility in identifying relevant supplying nodes across databases. The current implementation of GeoPolRisk in *edges* includes about 43,000 such definitions.

This example illustrates how exchange-resolved LCIA supports indicators that depend not only on the substance exchanged, but also on which node supplies and receives it, and where nodes are located—something not possible in traditional node-based approaches.

2.5.3 Use Case 3: Scenario-based Prospective LCIA with Parameterized CFs for Global Warming Potential

The third use case illustrates how exchange-resolved LCIA can incorporate parameterized and scenario-sensitive CFs, enabling prospective impact assessment.

This is particularly relevant when assessing impacts under varying future conditions, such as changing atmospheric greenhouse gas concentrations.

In this example, we consider concentration-dependent Global Warming Potential (GWP) CFs for methane (CH_4) and nitrous oxide (N_2O), following the physical formulation of Absolute Global Warming Potential (AGWP) as described in the IPCC AR6 Working Group I report and the future gas concentration values according to four Representative Concentration Pathways (RCP) developed by the IPCC, presented in Table 2 and sourced from the Annex III document (Intergovernmental Panel on Climate Change (IPCC) 2023).

Table 2: Gas concentration values for CH_4 (C_CH4) and N_2O (C_NO2). Concentration values for 2019 are used for 2020. RCP = Representative Concentration Pathways.

	C_CH_4 (ppb)			
RCP	1.9	2.6	4.5	8.5
2020	1866			
2050	1,428	1,519	2,020	2,446
2080	1,150	1,197	1,779	2,652
2100	1,036	1,056	1,683	2,415
	C_N_2O (ppb)			
RCP	1.9	2.6	4.5	8.5
2020	332			
2050	344	344	356	358
2080	350	349	373	380
2100	354	354	377	392

The CF is defined as a symbolic expression. Here is the case for CH_4:

```
{
  "supplier": {
    "name": "Methane, fossil",
    "operator": "contains",
    "matrix": "biosphere"
  },
  "consumer": {
    "matrix": "technosphere"
},
  "value": "GWP('CH4', H, C_CH4)"
}
```

This expression calls the external function `GWP()`, which takes the gas name, its background concentration (*C_CH4* for methane), and time horizon *H* as inputs. The function, detailed in the notebook included in the electronic SI material,

calculates the concentration-dependent GWP for the specified gas as the ratio of the gas's Absolute Global Warming potential (AGWP) to that of CO_2.

The resulting GWP CF values are dynamically inserted into the characterization matrix for each value pair provided for *H* and *C*. Parameters are externally supplied from climate scenarios (see Table 2), enabling consistent alignment between inventory modeling and evolving atmospheric conditions.

This approach supports prospective LCIA by allowing CFs to reflect the changing climate system. Rather than relying on fixed values (e.g., GWP100 = 28 for CH_4), users can explore how future CH_4 emissions may have stronger or weaker impacts based on projected concentrations.
By supporting symbolic CFs and parameterized evaluation, the exchange-based LCIA framework enables a close integration between LCA and integrated climate scenario modeling—an essential step toward robust, policy-relevant impact assessments.

2.5.4 Use Case 4: Scenario-based Prospective LCIA with Parameterized CFs for Fossil Fuels Scarcity

This use case illustrates how exchange-resolved LCIA can support prospective modeling of fossil resource scarcity, again using scenario-sensitive, parameterized CFs. Specifically, we implement a formulation of Surplus Cost Potential (SCP)—a measure of the additional cost incurred due to the depletion of fossil energy carriers (coal, oil, and natural gas)—whose value varies dynamically over time and across integrated assessment model (IAM) scenarios.

In the original ReCiPe 2016 implementation (Vieira et al. 2016), surplus production costs were derived from global average surplus extraction costs using static marginal cost increase (MCI) values per fossil fuel type (e.g., USD/GJ²). These MCIs were then combined with a fixed marginal extraction rate to calculate constant CFs (in USD/GJ), which were subsequently converted to USD/kg or USD/Nm³ via energy content assumptions. While this provides a consistent global midpoint indicator, it does not account for changing resource economics or energy demand trajectories under climate policy scenarios.

Our approach extends this formulation by parameterizing the CFs as symbolic expressions evaluated per year and scenario. The core expression is:

$$CF_t = \frac{MCI_t \cdot P_t}{5 \cdot (1 + d_t)}$$

where:

- MCI_t: the marginal cost increase of extraction for the given fossil fuel at time t (USD/GJ²), obtained from the derivative of the IAM-simulated extraction cost curve;
- P_t: the annual extraction volume (EJ/year), approximated from cumulative extraction data;
- d_t: the scenario-specific discount rate, reflecting time preference for future costs;
- The factor 5 annualizes the data in the scenario output, which is given with a time step of 5 years.

The CFs are evaluated in units of USD/GJ, then converted to USD/kg (for coal and oil) or USD/m³ (for natural gas) using representative energy contents. In *edges*, it is implemented the following way:

```
{
  "supplier": {
    "name": "Oil, crude",
    "categories": [
      "natural resource",
      "in ground"
    ],
    "matrix": "biosphere"
  },
  "consumer": {
    "matrix": "technosphere"
  },
  "value": "(MCI_OIL * P_OIL / 5) / (1 + d)"
}
```

Unlike the static approach of Vieira et al., our method retrieves scenario-specific time series for *MCI*, *P* (for each fuel), and *d* directly from IAM scenario outputs, allowing the CFs to evolve dynamically over time and across socio-economic pathways. The scenarios used in this study are based on the REMIND model v.3.5 (Luderer et al. 2020) and span a range of socio-economic pathways (SSP1–3) combined with climate policy assumptions, including near-term policy implementation (NPi, i.e., National Policies implemented), long-term carbon budgets (PkBudg650, i.e., 650 GtC of global carbon budget between 2022 to 2100), and a roll-back on previously committed investment in renewables (rollback). These scenarios represent contrasting futures regarding fossil fuel use, extraction dynamics, and mitigation ambition, providing a rich basis for evaluating how fossil resource scarcity impacts evolve.

3 Results

Results are presented for each of the use case presented above. Each features specific adaptations to meet the needs of the applied characterization models.

3.1 Use case 1: AWARE

Fig. 2 illustrates the LCA results for producing one kilogram of hydrogen via water electrolysis in France, using offshore wind power. The analysis resulted in ~8'800 exchanges associated with 512 unique CF values. From panel a), 50% (0.014 m^3) of the net freshwater use originates from the electrolysis itself in France, with the remaining 50% being consumed by other European countries (~10%), India (6% from the production of iron pellet and steel), South Africa (4%, from the mining of platinum used in the electrolyzer) and other countries (30%), for a total of 0.029 m^3. However, panel b) shows that the lowest water deprivation CF applies to French water consumers, while the highest applies to South African activities. Panel c) indicates that despite consuming only 4% of the freshwater in the system, the provision of water necessary for the extraction of platinum in South Africa is the most impactful process in the system once water scarcity is factored in, following the water needed for the electrolysis in France. It results in a total score of 0.62 m^3 world-eq. per kg of hydrogen with a 50% confidence interval of 0.45—0.71. Using the global default CF of 39.5 m^3 world-eq./m^3 would yield a total score of 1.17, overestimating the impact by 89%. The reader should note that 1) the CF applied to exchanges where the consuming process has the location RoW is exchange-specific: it averages 25 but ranges from 20 to 30; 2) only the uncertainty linked to using spatially aggregated CFs is considered; 3) using French grid electricity to power the electrolyzer would increase the share of water consumption occurring in France, primarily due to evaporation in hydro and nuclear power plants. However, this would obscure the significance of supply chain contributions, such as the water used for mining platinum and iridium.

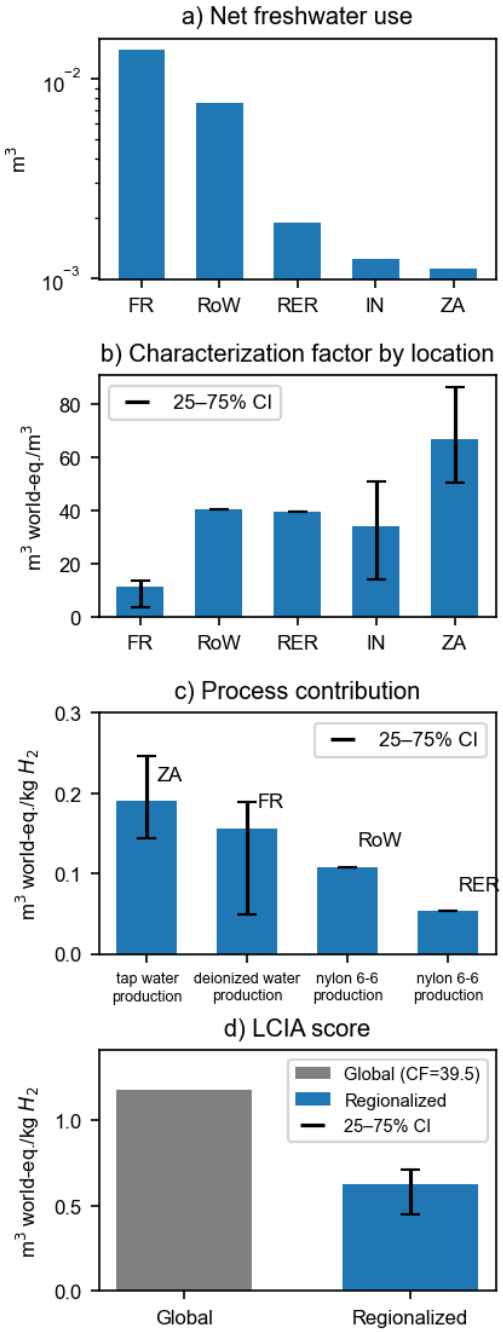

Fig. 2 – Water scarcity assessment for producing one kilogram of hydrogen from offshore wind power through water electrolysis in France, using AWARE 2.0. Values in panels c)

and d) are estimated using a Monte Carlo analysis over 10,000 iterations. Note that only the uncertainty associated with the spatial resolution of CFs is considered, not that stemming from inventories. a) Net freshwater use per consumer location (five largest), measured in cubic meters. Net use indicates the difference between water uptake and release. b) Mean and 25-75th percentiles CF values per consumer location, represented in cubic meters of deprived freshwater per cubic meter of net freshwater use. Note that composite regions (e.g., RoW) do not carry uncertainty. c) Characterized contribution of the four most relevant processes, in reference to one kg of hydrogen produced, in cubic meters of deprived freshwater. d) Comparison of the total score using a global CF value of 39.5 and region-specific CF values.

3.2 Use case 2: GeoPolRisk

Fig. 3 presents the inventory results for assessing geopolitical supply risk associated with producing one kilogram of electrolytic hydrogen in France using offshore wind power.

Panel a) shows the resources most consumed in terms of mass, relative to the functional unit. Coal is the largest input by weight, followed by pig iron, petroleum, and natural gas. These results reflect the upstream material requirements embedded in the construction and operation of offshore wind infrastructure, electricity transmission, and hydrogen production systems.

Panel b) highlights the resources with the highest average CFs for geopolitical supply risk, calculated as the total impact divided by the total amount required for each resource. Platinum and iridium, primarily sourced from South Africa and Russia, rank highest, reflecting their geopolitical sensitivity due to concentrated global supply.

Panel c) illustrates how *edges* enables the application of CFs specific to supplier-consumer location pairs for a given resource, exemplified here with crude petroleum.

Finally, panel d) combines the amount of each resource used and its associated CF, broken down by supplier-consumer location pairs. This reveals the main contributors to the total geopolitical supply risk, with bauxite, hard coal, ferronickel, and pig iron emerging as the most critical, due to their volume and moderate to high CFs. Iridium also appears among the top contributors despite its low absolute use–only about 1 microgram per kilogram of hydrogen. This highlights the importance of materials with high CFs, which capture supply concentration and governance risks, even when such materials are used in very small quantities.

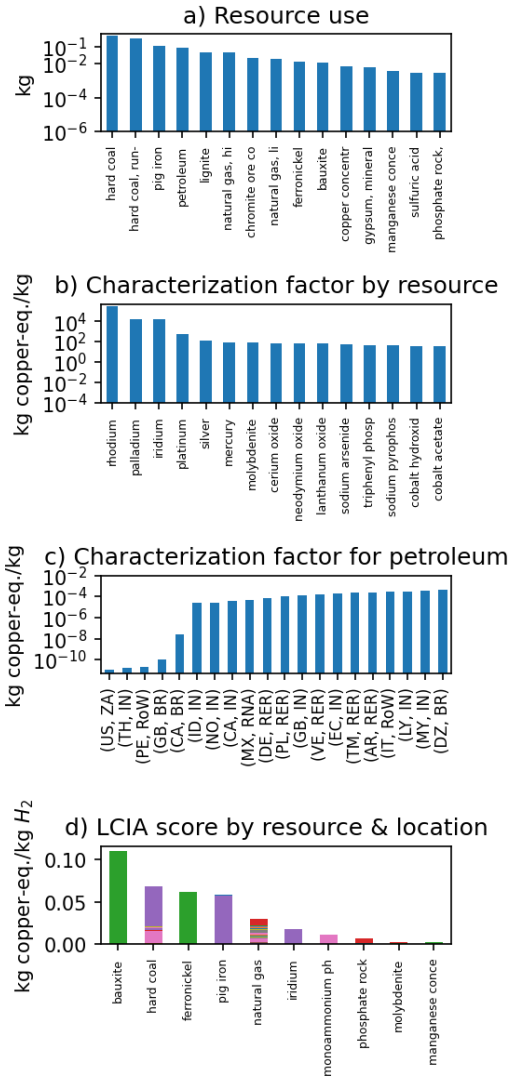

Fig. 3 – Geopolitical supply risk associated with resource use for producing one kilogram of electrolytic hydrogen in France, based on GeoPolRisk 1.0. Y-axes of top, second, and fourth panels use logarithmic scales. a) Mass of each resource used (in kilograms). b) Weighted average CF applied per resource, in kg copper-eq./kg. c) Weighted average CF for petroleum, for different pairs of supplier-consumer locations, in kg copper-eq./kg. d) Ten most critical abiotic resource traded, by supplier location, in kg copper-eq/kg hydrogen. Each color represents a geographical origin. Note that the average CF values displayed in b) and c) are weighted by the amounts of the exchanges involved in the system. Hence, they are specific to this case.

3.3 Use case 3: Global Warming Potential

Fig. 4 presents the evolution of the CFs for GWP and corresponding scores to produce one kg of electrolytic hydrogen in France using offshore wind power, under four RCP scenarios (RCP2.6, RCP4.5, RCP6.0, and RCP8.5) for the period 2025–2100. Note that this example does not consider any changes in the hydrogen production system (e.g., the efficiency of the electrolyzer, the electricity mix, etc.), but only changes in the GHG atmospheric concentrations. Panel a) illustrates the concentration-dependent GWP factors (expressed in kg CO_2-equivalents per kg emission) for the two major greenhouse gases: methane (CH_4) and nitrous oxide (N_2O). Results demonstrate that the GWP factors for CH_4 and N_2O vary across scenarios due to changes in the gases' background concentrations, which affect their relative radiative efficiencies and lifetimes compared to CO_2. Carbon dioxide retains a constant GWP factor of 1, as it is the reference substance.

Specifically, in low-emission pathways such as RCP2.6, the reduced atmospheric burden leads to higher radiative efficiencies per molecule, thereby increasing the GWP CFs values relative to those in high-emission pathways.

The bottom panel of Fig. 4 shows the total GWP-based LCIA score per kilogram of electrolytic hydrogen produced over time. Logically, under the RCP2.6 scenario, the overall climate change impact score increases with time, while in the higher-emission scenarios (RCP6.0 and RCP8.5), the score decreases. This counterintuitive trend results from the stronger climate forcing exerted by marginal emissions of CH_4 and N_2O under cleaner atmospheric conditions, as captured by the concentration-dependent GWP CFs formulation. In this case, the variation of scores across scenarios remains modest, as the system emits low amounts of CH_4 and N_2O relative to CO_2, unlike other systems (e.g., agricultural activities).

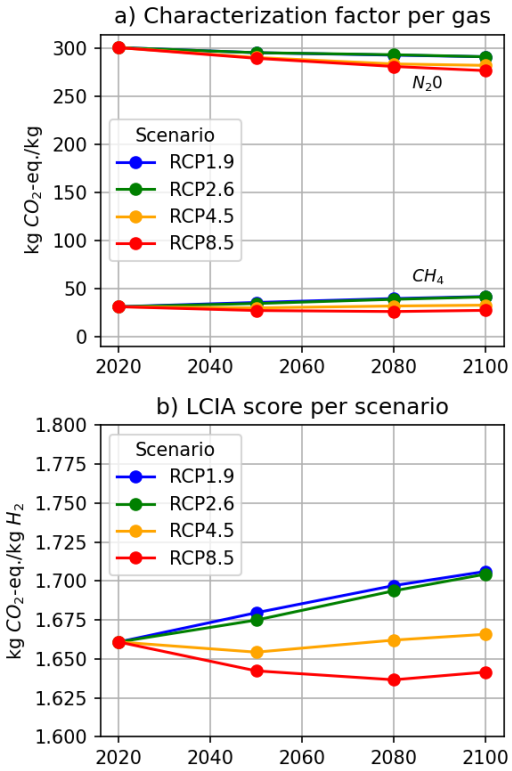

Fig. 4 – Evolution of concentration-dependent Global Warming Potential (GWP) factors and scores under four RCP scenarios (RCP2.6, RCP4.5, RCP6.0, RCP8.5) between 2025 and 2100. a) GWP CFs for CH_4, and N_2O, in kg of CO_2-eq. per kg of emission. b) Total GWP score per kg of hydrogen across the four RCP scenarios. Lower atmospheric concentrations in mitigation pathways lead to higher radiative efficiencies and increased impact scores.

3.4 Use case 4: Fossil Fuels Scarcity

Results shown in Fig. 5 indicate a clear relationship between scenario assumptions and the CFs for fossil fuel scarcity. In stringent mitigation scenarios like SSP1-PkBudg650, fossil fuel extraction volumes (*P*) decline rapidly due to strong climate policies and low-carbon transitions. This, in turn, limits the rate at which cumulative resources are depleted, leading to more moderate increases in marginal extraction costs (*MCI*). Additionally, such scenarios often feature higher or more stable discount rates (*d*), further dampening the resulting CFs. These factors yield CFs that decrease significantly over time, reflecting

a lower scarcity pressure under strong mitigation. Conversely, in scenarios with delayed or weak climate action—such as SSP3-rollBack—extraction volumes remain high or even grow, driving up cumulative depletion and leading to steeper marginal cost increases (higher *MCI*). Coupled with moderate discounting, this raises CFs over time, capturing the increased scarcity and cost burden of fossil resource use. These dynamics are directly encoded in the parameterized CF formulation. The influence of scenario trajectories on CF parameters is reflected in the LCIA impact scores: pathways with rapid fossil phase-out show a steep decline in impacts. In contrast, fossil-reliant pathways maintain high and persistent scores. This demonstrates the strength of using scenario-based, dynamic CFs in prospective LCA to reflect fossil fuel use's evolving cost and scarcity implications under different socio-economic and climate policy futures.

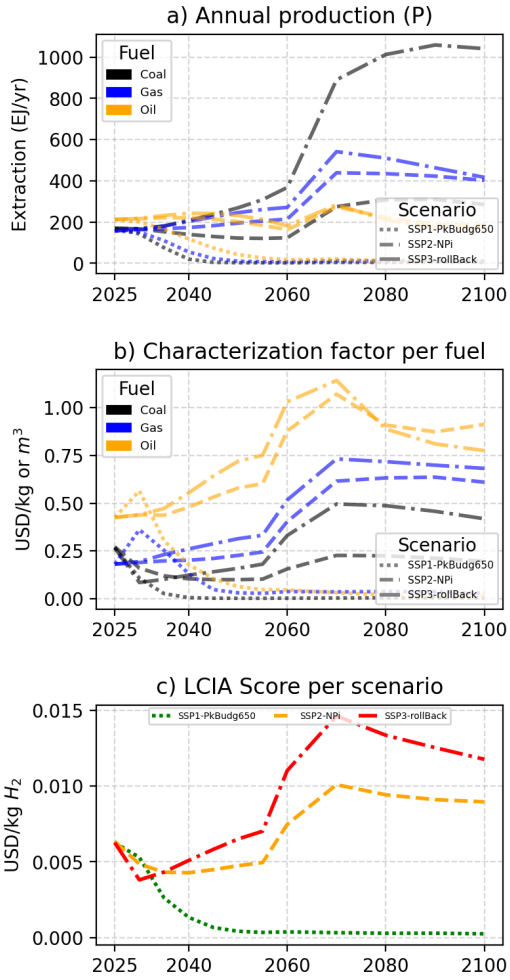

Fig. 5 – Surplus Cost of Fossil Fuel Extraction across three scenarios from REMIND v.3.5. a) Annual extraction rate, in exajoules (EJ), for hard coal, natural gas, and crude oil across multiple scenarios. b) Surplus cost potentials (SCP) per unit of resource (USD/kg for oil and coal, USD/Nm³ for gas) across multiple scenarios. c) Resulting LCIA scores per kilogram of electrolytic hydrogen across multiple scenarios. In a) and b), each line corresponds to a scenario, and each colour corresponds to a fuel. In c), each line corresponds to a scenario.

4 Discussion

This study introduced an exchange-resolved approach to LCIA, shifting the characterization from node-level elementary flows to exchanges between activities. Through four use cases, we demonstrated the flexibility and applicability of this method for regionalized, technosphere-aware, and prospective environmental assessments.

The results confirm that exchange-based LCIA can account for key spatial, relational, and scenario-dependent aspects of environmental impacts, offering a lower-overhead alternative to GIS-based modeling—albeit with less spatial granularity. By treating exchanges as the unit of impact characterization, the framework enables consistent modeling across various impact categories that depend on contextual parameters, including geographic location, supplier-consumer relationships, and evolving background conditions such as atmospheric GHG concentrations.

The regionalized water scarcity impact assessment (AWARE) illustrated how geographic disaggregation can be achieved without proliferating elementary flows or requiring manual flow duplication. Furthermore, we demonstrated that exchanges could be distinguished based on the consumer's location and CPC category. The technosphere-based supply risk assessment (GeoPolRisk) further showed that impacts can depend on the supply chains' structure, which 1) increases flexibility for applying the LCIA method and 2) introduces a relational dimension that traditional LCIA does not capture. Finally, the prospective GWP and fossil fuels examples demonstrated that concentration- and scenario-dependent characterization factors can be dynamically evaluated, aligning LCA outputs more closely with integrated scenario modeling frameworks such as RCPs or SSPs.

However, this approach also presents limitations. First, as already noted by C. L. Mutel & Hellweg (2009), implementing regionalized indicators at the national or sub-national level cannot possibly capture site-specific impacts. Environmental conditions, such as water scarcity, ecosystem sensitivity, air quality, and population density, vary widely within a country. This is the reason why indicators like AWARE define CFs at the watershed level. However, one may try to overcome this issue by explicitly modelling the uncertainty introduced by using aggregated CFs and letting it propagate to the score level, as we did by integrating variability across watersheds (although it does not include uncertainty at the watershed level itself). Yet, suppose site-specific impacts are

expected to be of primary concern. In that case, using geo-referenced inventories coupled with tools to model fate, exposure, and effect based on real-world environmental data (e.g., local hydrology models for water impacts, air dispersion models for air pollution) is preferable. Second, despite efficient implementation and advanced matching algorithms, the *edges* library requires a few seconds to a few minutes to calculate a score, compared to a fraction of a second for *brightway2-calc*, as it needs to verify the eligibility of every exchange involved in the inventory matrix (which can amount to several hundreds of thousands). Third, while the method supports regionalization and parameterization, it relies on the availability and quality of relevant metadata (e.g., locations, classifications) in inventories and characterization factor definitions. Limited trade data, gaps in inventory geographies, or inconsistencies in metadata are frequent in common LCA databases. They can lead to reduced model fidelity. There is however a clear trend in spatializing inventory databases, as demonstrated by (Peng and Pfister 2024) and, more recently, by the development of *regioinvent* (Agez 2025). Coupling their use with *edges* could provide more accurate assessments. Finally, while symbolic CFs allow flexible prospective modeling, the quality of the results ultimately depends on the robustness of the underlying parameterizations (e.g., GWP models, concentration scenarios).

Future research could expand exchange-resolved LCIA in several directions. First, while *edges* already implements AWARE, IMPACT World+, and GeoPolRisk, a broader application to other regionalized or relational impact assessment methods could further demonstrate its generalizability. Second, using complex external models to evaluate CFs, as shown (to a limited extent) with the GWP example, is promising. One could envision calling an external API to retrieve current atmospheric conditions to calculate the marginal contribution to air pollution for different substances. Third, future work could explore the coupling of exchange-resolved LCIA with forward-looking inventory models, in which both the life cycle foreground system and background environmental conditions co-evolve. It offers a good framework to operationalize existing prospective LCIA methods, such as those proposed for water scarcity (Núñez et al. 2015; Baustert et al. 2022), ozone depletion (van den Oever et al. 2024), impacts on biodiversity from land use (de Baan et al. 2013), and impacts on freshwater ecosystems from climate change and water consumption (Hanafiah et al. 2011; Cosme and Niero 2017). This would open the door to assessments where changes in supply chains, technology mixes, or infrastructure are dynamically matched with corresponding shifts in characterization factors, improving the consistency and relevance of prospective LCA studies. Finally, this work highlights the potential of more dynamic LCIA frameworks, and we encourage LCA

software developers (e.g., SimaPro, OpenLCA, and Activity Browser) to consider supporting such approaches in the future to better capture the spatial, temporal, and parametric complexity of impact assessment.

In summary, exchange-based LCIA represents a pragmatic and scalable advancement for context-sensitive environmental assessment. It occupies an essential methodological space between conventional node-based LCIA and fully spatially explicit, GIS-integrated models. It provides a robust yet accessible solution for regionalized, relational, and prospective life cycle assessments.

Data Availability

The distributable form of the Python library used to produce the results presented in this article is freely available from the Python Package Index (PyPI). Its source code is available in the following repository: https://github.com/Laboratory-for-Energy-Systems-Analysis/edges. Documentation is available at this address: https://edges.readthedocs.io/en/latest/. Scripts to reproduce the use cases presented in this article are provided as Electronic Supplementary Material documents.

References

Agez M (2025) Regioinvent https://doi.org/10.5281/zenodo.11836125

Baustert P, Igos E, Schaubroeck T, et al (2022) Integration of future water scarcity and electricity supply into prospective LCA: Application to the assessment of water desalination for the steel industry. J Ind Ecol 26:1182–1194. https://doi.org/10.1111/jiec.13272

Boulay AM, Bare J, Benini L, et al (2018) The WULCA consensus characterization model for water scarcity footprints: assessing impacts of water consumption based on available water remaining (AWARE). Int J Life Cycle Assess 23:368–378. https://doi.org/10.1007/s11367-017-1333-8

Bulle C, Margni M, Patouillard L, et al (2019) IMPACT World+: a globally regionalized life cycle impact assessment method. Int J Life Cycle Assess 24:1653–1674. https://doi.org/10.1007/s11367-019-01583-0

Cosme N, Niero M (2017) Modelling the influence of changing climate in present and

future marine eutrophication impacts from spring barley production. J Clean Prod 140:537–546. https://doi.org/10.1016/j.jclepro.2016.06.077

de Baan L, Mutel CL, Curran M, et al (2013) Land Use in Life Cycle Assessment: Global Characterization Factors Based on Regional and Global Potential Species Extinction. Environ Sci Technol 47:9281–9290. https://doi.org/10.1021/es400592q

Francesca Verones, Stefanie Hellweg, Assumpcio Anton, et al (2020) LC-IMPACT: A regionalized life cycle damage assessment method. J Ind Ecol 24:1201–1219

Gemechu ED, Helbig C, Sonnemann G, et al (2016) Import-based Indicator for the Geopolitical Supply Risk of Raw Materials in Life Cycle Sustainability Assessments. J Ind Ecol 20:154–165. https://doi.org/10.1111/jiec.12279

Gerloff N (2021) Comparative Life-Cycle-Assessment analysis of three major water electrolysis technologies while applying various energy scenarios for a greener hydrogen production. J Energy Storage 43:. https://doi.org/10.1016/j.est.2021.102759

Gonzales-Calienes G, Kannangara M, Yang J, et al (2022) Life cycle assessment of hydrogen production pathways in Canada

Hanafiah MM, Xenopoulos MA, Pfister S, et al (2011) Characterization Factors for Water Consumption and Greenhouse Gas Emissions Based on Freshwater Fish Species Extinction. Environ Sci Technol 45:5272–5278. https://doi.org/10.1021/es1039634

Hauschild MZ, Potting JJ (2005) Spatial differentiation in Life Cycle impact assessment - The EDIP2003 methodology-Guidelines from the Danish Environmental Protection Agency. Danish Environ Prot Agency

Heijungs R, Suh S (2002) The Computational Structure of Life Cycle Assessment. , Lon_don

Intergovernmental Panel on Climate Change (IPCC) (2023) Annex III: Tables of Historical and Projected Well-mixed Greenhouse Gas Mixing Ratios and Effective Radiative Forcing of All Climate Forcers

Koyamparambath A, Loubet P, Young SB, Sonnemann G (2024) Spatially and temporally differentiated characterization factors for supply risk of abiotic resources in life cycle assessment. Resour Conserv Recycl 209:107801. https://doi.org/10.1016/j.resconrec.2024.107801

Li J, Tian Y, Zhang Y, Xie K (2021) Spatializing environmental footprint by integrating geographic information system into life cycle assessment: A review and practice recommendations. J Clean Prod 323:129113. https://doi.org/10.1016/j.jclepro.2021.129113

Luderer G, Bauer N, Baumstark L, et al (2020) REMIND - REgional Model of INvestments and Development - Version 2.1.3. In: https://www.pik-potsdam.de/research/transformation-pathways/models/remind

Mutel C (2017) Brightway: An open source framework for Life Cycle Assessment. J Open Source Softw 2:236. https://doi.org/10.21105/joss.00236

Mutel C, Liao X, Patouillard L, et al (2019) Overview and recommendations for regionalized life cycle impact assessment. Int J Life Cycle Assess 24:856–865. https://doi.org/10.1007/s11367-018-1539-4

946 Mutel CL, Hellweg S (2009) Regionalized life cycle assessment: Computational
947 methodology and application to inventory databases. Environ Sci Technol 43:5797–
948 5803. https://doi.org/10.1021/es803002j
949 Mutel CL, Pfister S, Hellweg S (2012) GIS-based regionalized life cycle assessment: How
950 Big is small enough? Methodology and case study of electricity generation. Environ
951 Sci Technol 46:1096–1103. https://doi.org/10.1021/es203117z
952 Núñez M, Pfister S, Vargas M, Antón A (2015) Spatial and temporal specific
953 characterisation factors for water use impact assessment in Spain. Int J Life Cycle
954 Assess 20:128–138. https://doi.org/10.1007/s11367-014-0803-5
955 Peng S, Pfister S (2024) Regionalizing the supply chain in process life cycle inventory with
956 multiregional input–output data: An implementation for ecoinvent with EXIOBASE.
957 J Ind Ecol 28:680–694. https://doi.org/10.1111/jiec.13491
958 Seitfudem G, Berger M, Schmied HM, Boulay A (2025) The updated and improved method
959 for water scarcity impact assessment in LCA, AWARE2.0. J Ind Ecol.
960 https://doi.org/10.1111/jiec.70023
961 Seppälä J, Posch M, Johansson M, Hettelingh JP (2006) Country-dependent
962 characterisation factors for acidification and terrestrial eutrophication based on
963 accumulated exceedance as an impact category indicator. Int J Life Cycle Assess
964 11:403–416. https://doi.org/10.1065/lca2005.06.215
965 Simoes SG, Catarino J, Picado A, et al (2021) Water availability and water usage solutions
966 for electrolysis in hydrogen production. J Clean Prod 315:128124.
967 https://doi.org/10.1016/J.JCLEPRO.2021.128124
968 Smolinka T, Wiebe N, Sterchele P, et al (2018) Industrialisierung der Wasserelektrolyse in
969 Deutschland: Chancen und Herausforderungen für nachhaltigen Wasserstoff für
970 Verkehr, Strom und Wärme
971 van den Oever AEM, Puricelli S, Costa D, et al (2024) Revisiting the challenges of ozone
972 depletion in life cycle assessment. Clean Environ Syst 13:100196.
973 https://doi.org/10.1016/j.cesys.2024.100196
974 Vieira MDM, Ponsioen T, Goedkoop M, Huijbregts MAJ (2016) Fossil resource scarcity. In:
975 ReCiPe 2016. A harmonized life cycle impact assessment method at midpoint and
976 endpoint level. Report I: Characterization. pp 95–118
977 Wernet G, Bauer C, Steubing B, et al (2016) The ecoinvent database version 3 (part I):
978 overview and methodology. Int J Life Cycle Assess 21:1218–1230.
979 https://doi.org/10.1007/s11367-016-1087-8
980 Yang Y, Heijungs R (2017) A generalized computational structure for regional life-cycle
981 assessment. Int J Life Cycle Assess 22:213–221. https://doi.org/10.1007/s11367-016-
982 1155-0
983

Acknowledgments

The authors acknowledge the financial support of the French energy agency ADEME through the HySPI project (nr. 2197D0085): Hydrogène industriel – Scénarios Prospectifs des Impacts environnementaux. The HySPI project aims to provide a methodological framework to analyze and quantify the environmental impacts of the decarbonization strategy for hydrogen production used by the industry in France systematically and prospectively. The authors also acknowledge the financial support of the Europe Horizon project RAWCLIC (project ID 101183654) and that of the Europe Horizon project PRISMA (project ID 101081604). Finally, the authors would like to thank Juliana Steinbach from Mines Paris PSL for the constructive discussion.

Competing Interests

The authors declare no conflict of interest.

Supplementary Information

Scripts to reproduce the results presented in the four use cases are available as supplementary information.

- Life cycle inventories for hydrogen production
- Link to notebook for use case 1
- Link to notebook for use case 2
- Link to notebook for use case 3
- Link to notebook for use case 4

Contributions

Romain Sacchi: Conceptualization, Methodology, Software, Writing - Original draft preparation. Alvaro Hahn Menacho: Methodology, Data curation, Writing - Review & Editing. Georg Seitfudem, Maxime Agez, and Anish Koyamparambath: Data curation, Writing - Review & Editing. Joanna Schlesinger, Jair Santillan Saldivar, Philippe Loubet, and Christian Bauer: Writing - Review & Editing